Engineering Research Journal
journal homepage: https://erj.journals.ekb.eg/

Experimental Study on the Shear Transfer of Composite Beams with Top Layer Using Different Shear Dowels Distribution

Ehsan Nabil[1,*], Mohamed Yehia[1], Nehal Magdy[1], Alaa Sherif[1]

[1] Civil Engineering Department, Faculty of Engineering Mataria, Helwan University, Cairo, Egypt
*Corresponding author E-mail: ehsannabil2018@gmail.com

Abstract. The interfacial shear behavior of composite concrete beams is a critical factor influencing their overall structural performance and load-carrying capacity. When an additional concrete layer is added to an existing beam for strengthening purposes, the bond and shear transfer between the two layers play a crucial role in ensuring effective composite action. The interfacial shear capacity depends on factors such as surface preparation, material properties, and the presence of shear connectors. Shear connectors, including dowels, studs, or roughened surfaces, help enhance load transfer and prevent premature failure due to delamination. The distribution and spacing of these connectors significantly affect the beam's strength and ductility. Two primary methods are commonly used to evaluate interfacial shear strength: one based on the maximum compressive forces at mid-span and the other on peak shear flow at the beam supports. Research has shown that concentrating shear connectors near the supports can improve ductility and prevent slip at the interface. Experimental studies have been conducted to better understand the shear transfer mechanisms and optimize design approaches. These studies have led to simplified analytical models for predicting interfacial shear capacity, validated through experimental results. Proper assessment and design of interfacial shear behavior are essential to ensure the ductility and efficiency of strengthened composite concrete beams.

Keywords: Interfacial shear, Ductility, Shear connectors, Shear flow.

1 Introduction

Composite concrete flexural members are widely used in structural applications such as buildings and bridges due to their ability to combine different materials for enhanced performance. Achieving effective composite action requires reliable shear connections between the existing and newly cast concrete layers. Various methods, including rough surface interfaces, shear keys, steel dowels, and epoxy bond-

DOI: 10.21608/erj.2025.384077.1238
Received 18 May 2025; Received in revised form 04 June 2025; Accepted 26 June 2025
Available online 01 September 2025

ing, are used to ensure interfacial integrity. The shear transfer strength is influenced by numerous factors such as concrete strength, span-depth ratio, layer slip, interface position relative to the neutral axis, aggregate properties, and dowel distribution. Previous studies have shown that rough interfaces can retain up to 87% of monolithic slab strength [14], and uniformly distributed dowels improve performance more than perimeter-only arrangements, even with equal total dowel areas [14]. Additionally, slabs with interfaces below the neutral axis exhibit 10–20% greater shear capacity compared to those above it [12–13]. Other research [1, 2, 3–11] has further explored shear behavior, with [8] and [9–11] examining shear transfer mechanisms in detail.

Recent work has extended this investigation to high-performance materials. Yang Song [28] demonstrated that applying ultra-high-performance concrete (UHPC) to over-reinforced beams improved load capacity by 88.1% and achieved a ductility coefficient of 23.85. Liu et al. [29,30] found that UHPC layers of up to 80 mm thickness, combined with closely spaced shear anchors (<300 mm), significantly enhanced the stiffness and shear resistance of T-beams, especially when U-shaped jackets were used. These findings underscore the importance of effective interfacial shear transfer, particularly under service loads where significant stresses develop. Without adequate shear connectors, the composite system fails to act monolithically. Structural codes such as AASHTO, ACI, and CSA [15–17] provide design guidelines based on either maximum compressive force at mid-span or maximum shear at supports. In this context, the current study experimentally examines six composite beams comprising a precast lower part and a cast-in-place upper concrete layer with varying shear connector arrangements. All specimens were tested under monotonic static loading until failure to evaluate the influence of connector distribution on composite behavior.

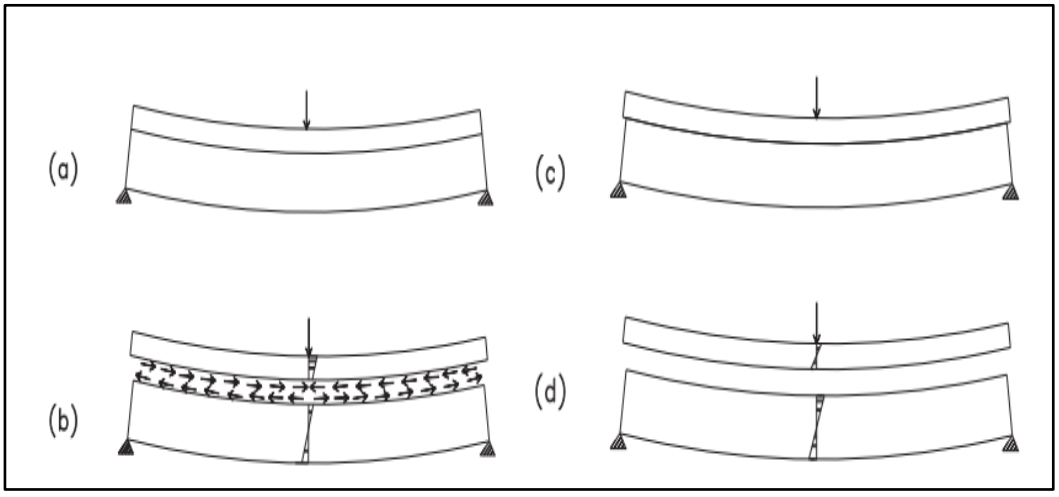

Fig. 1 (a) Fully composite section, (b) interfacial shear transfer in composite section, (c) horizontal slip, (d) non-composite section.

2 Experimental Program.

The experimental study involved testing six reinforced concrete beams. Five of these beams featured a two-layer construction, with a 350 mm thick lower layer, a 50 mm thick upper layer, a width of 150 mm, and an overall span of 2100 mm. The sixth beam, labeled B01, served as a control and was built as a single-layer beam with a 400 mm thickness, omitting the upper layer. All beams were simply supported, with a clear span of 1800 mm. The main reinforcement used in all beams consisted of two 16 mm diameter

bars, while the top layer reinforcement included two 12 mm diameter bars. For transverse reinforcement, steel stirrups of 10 mm diameter at a spacing of 5 per meter were used—running through both layers in the control beam (B01) and only through the bottom layer in the other beams. The beams were loaded until failure as part of the testing process, which aimed to examine the impact of horizontal shear forces and to evaluate the performance of a specific strengthening method. The outcomes for the strengthened beams are discussed separately in a study by Awry et al. [23]. The test beams varied in terms of shear connector configurations, including differences in reinforcement area and connector distribution. Beam B02 had no shear connectors but featured a roughened surface for the upper concrete layer. Beams B03 and B04 included shear connectors with identical reinforcement areas but differed in bar diameter and spacing. Beams B05 and B06 also had the same total reinforcement area, but their shear connectors were arranged differently, being concentrated at the beam ends. Details of the beam configurations are summarized in Table 1 and illustrated in Figure 2.

Table 1 Matrix of tested beams.

Beam ID	Reinforcement					
	Bottom Rft.	Top Rft.	Stirrups	fy of shear connectors (MPa)	Shear Connectors	
					Zone-1 550 mm	Zone-2 1000 mm
B01	2Ø16	2Ø12	5Ø10/m	–	Monolithic Construction	
B02	2Ø16	2Ø12	5Ø10/m	–	Roughness Surface	
B03	2Ø16	2Ø12	5Ø10/m	500	Ø10@400mm	
B04	2Ø16	2Ø12	5Ø10/m	300	Ø8@150mm	
B05	2Ø16	2Ø12	5Ø10/m	500	Ø10@300mm	Ø10@500mm
B06	2Ø16	2Ø12	5Ø10/m	300	Ø8@100mm	Ø8@200mm

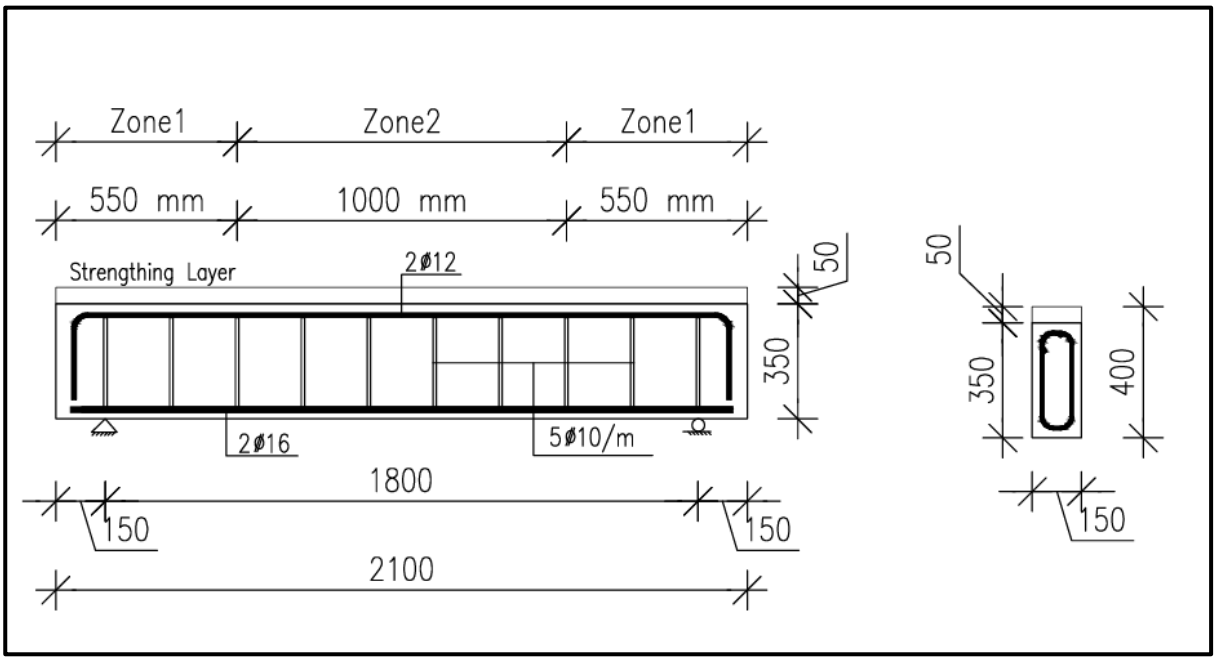

Fig. 2 Typical details of tested beams.

2.1 Test set-up, instrumentation and loading

The beams were tested under a progressively increasing vertical load, applied using a hydraulic jack with a 700-kN capacity. The load was measured using a load cell of the same capacity. A four-point loading setup was implemented with the help of steel I-beams, as depicted in Figure 3. Displacements were tracked using linear variable displacement transducers (LVDTs), offering a precision of 0.01 mm. Strain in both the concrete and steel reinforcement was recorded using 120-ohm steel strain gauges. Data was collected through a data acquisition system integrated with "LAB VIEW" software, operating at a sampling rate of one reading per second. Figure 4 shows the layout of the LVDTs and strain gauges for a typical beam. The mechanical properties of the materials and reinforcing bars are provided in Tables 2 and 3.

Fig. 3 Test set-up for the beams.

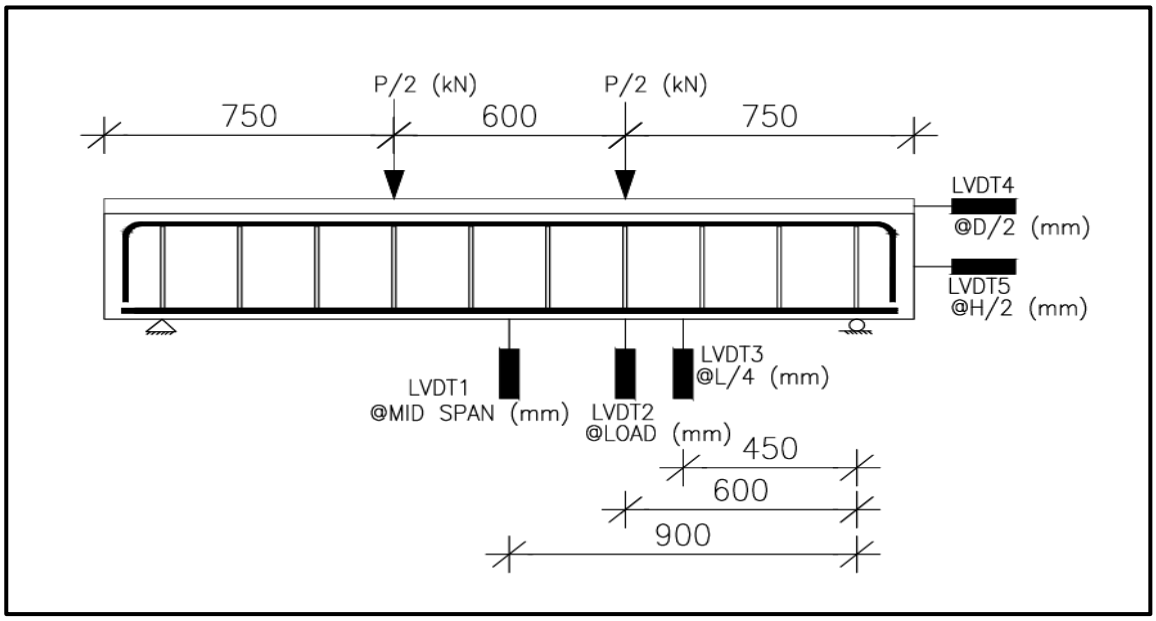

Fig. 4 Instrumentation for the tested beams.

Table 2: Material properties and mixing ratios of upper layer and lower concrete

Item	F_{cu} (MPa)	Ft (MPa)	Ec	v
Value	24.0	2.27	31553	0.2

Table 3: Mechanical properties of rebar.

Rebar	Diameter (mm)	Elasticity modulus	Poisson's ratio	Yield strength
Stirrup	10	200	0.3	500
Compression rebar	12	200	0.3	500
Tension rebar	16	200	0.3	500
Connector ф10	10	200	0.3	500
Connector ф 8	8	200	0.3	300

3 Experimental results and discussion

3.1 Experimental observations and crack pattern

All beams were tested until failure, with monitoring starting from the appearance of the first horizontal crack at the interface between the upper and lower concrete layers. This initial cracking was followed by the formation of shear and flexural cracks in the lower layer. Ductility was evaluated by calculating the ratio of two areas under the load–strain curve. The first area, A1, corresponds to the curve from zero load up to the elastic peak load, while the second area, A2, covers the portion from the elastic peak to either the failure load or 80% of the maximum load, whichever is greater. The elastic peak load was identified by locating the intersection point between the initial ascending slope of the curve and a horizontal line at the maximum load level, as shown in Figure 5. The ductility factor for each beam was calculated using Equation (1) and is summarized in Table 4. This factor reflects the beams' ability to undergo inelastic deformation. Table 4 also includes the experimental findings for each beam, along with the corresponding failure modes, which were determined based on observed cracking behavior, especially interfacial shear cracks. The failure modes and crack patterns for all tested beams are illustrated in Figures 6a to 6f.

Ductility Factor =A2 /A1 eq. (1)

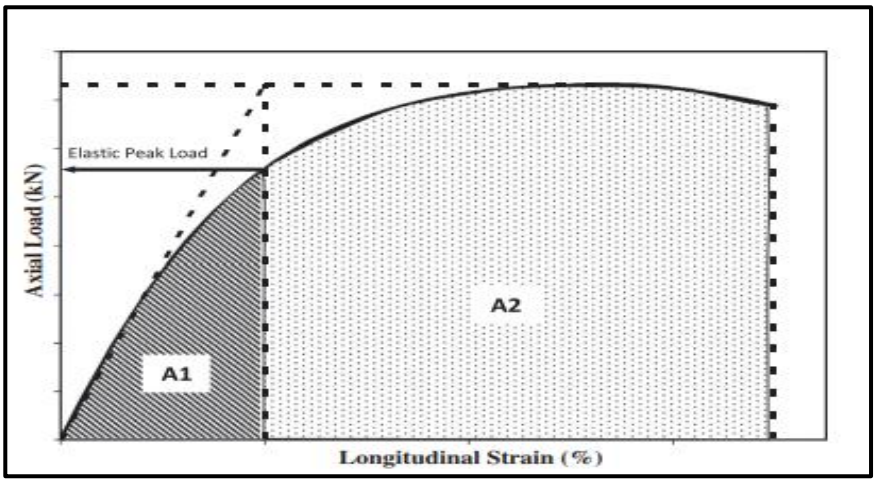

Fig. 5. definition of ductility

Table 4 Results of tested beams.

Beam ID	Failure P_{ult}	Δult	Pmax	Δmax	Py	Δy	Ductility Factor	Failure mode shape
B01	234.1	30.1	243.0	16.5	198.0	3.7	8.1	Flexural Failure
B02	212.5	27.5	220.0	22.0	161.5	5.0	5.5	shear flex-ural cracks
B03	228.0	28.0	233.1	20.0	180.0	4.4	6.4	shear flex-ural cracks
B04	233.4	29.5	236.8	19.7	186.0	4.5	6.6	shear flex-ural cracks
B05	227.4	28.5	228.4	20.4	205.9	4.4	6.5	shear flex-ural cracks
B06	232.4	30.0	235.6	19.8	180.0	4.5	6.7	shear flex-ural cracks

(a) – Failure of B01

(b) – Failure of B02

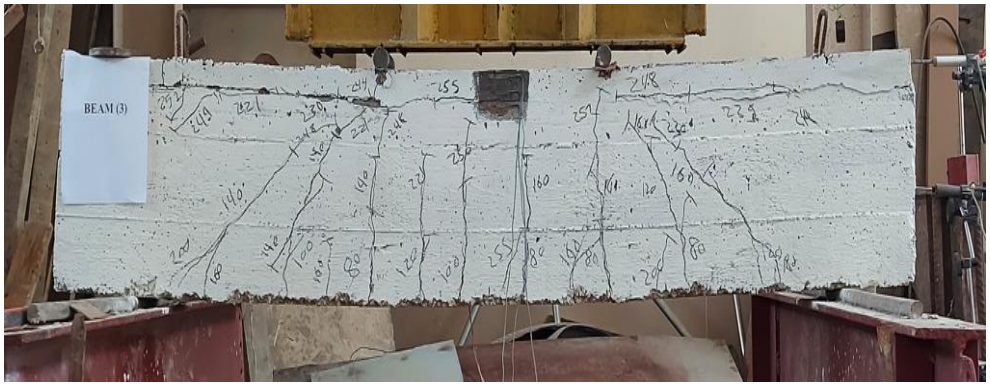

(c) – Failure of B03

(d) – Failure of B04

(e) – Failure of B05

(f) – Failure of B06

Fig. 6. Cracking pattern at failure for the tested beams

3.2 Discussion of the experimental results

3.2.1 Vertical deflection Characteristics

Beams B03 and B04 were strengthen with shear connectors evenly distributed along their spans, whereas in beams B05 and B06, the connectors were concentrated near the supports. For all four beams, the shear connector ratio was maintained at 0.20% using Ø10 mm and Ø8 mm connectors, respectively. The beams were designed to have equivalent flexural capacity and were compared against a control beam. Analyzing the mid-span load–deflection curves shown in **Figures 7a, 7b, and 7c**, it can be observed that beams B03, B04, B05, and B06—although reinforced with an additional layer and the same total area of shear reinforcement (differing only in connector diameter, distribution and spacing)—exhibited similar behavior up to failure. However, beams B03 and B05 demonstrated greater deflection under the same load compared to B01 and their counterparts B04 and B06, respectively. Ultimate load capacities were recorded as approximately 237 kN for B04 and 233 kN for B03, corresponding to 97.5% and 96% of the strength of the control (monolithic) beam. For B05 and B06, the ultimate capacities were around 228.5 kN and 235.6 kN, which equate to 94% and 97% of the monolithic beam's capacity. These findings indicate that while the composite action between layers was effective, it did not match the strength of a monolithic structure. Beams with Ø8 mm shear connectors showed higher stiffness and lower deflection than those with Ø10 mm connectors. This is attributed to the increased number of Ø8 mm connectors, which enhanced load distribution and minimized deformation. Furthermore, beams with Ø10 mm connectors displayed reduced ductility compared to those with Ø8 mm ones. The smaller diameter connectors allowed for more deformation prior to failure, improving the beam's energy absorption under load. The strategy of concentrating connectors near the supports—where shear forces are greatest—significantly improved ductility. This approach enhanced the clamping action between the two layers, minimizing slippage and improving the beam’s deformation capacity. Maximum slip was observed at the beam ends, while slip at the mid-span remained negligible, confirming that concentrating connectors at the ends effectively controlled interlayer movement.

Figures 7d show the load versus mid-span deflection behavior for beams B01, B02, and B03 up to failure. Beam B03, which was reinforced with shear connectors, demonstrated a more efficient load-bearing response. The shear connectors effectively distributed the applied load between the two layers,

minimizing stress concentrations and enhancing the beam's capacity. By creating a more rigid connection between the layers, the connectors improved vertical stiffness, reducing deflections and ensuring composite action—where both layers deform together rather than independently. In contrast, beam B02 relied solely on friction between the layers, with no shear connectors. While friction allowed some degree of load transfer, it was less effective, resulting in uneven load distribution and localized stress concentrations under higher loads. The limited interlayer resistance in B02 led to reduced overall stiffness, increasing the risk of instability under heavy loading conditions.

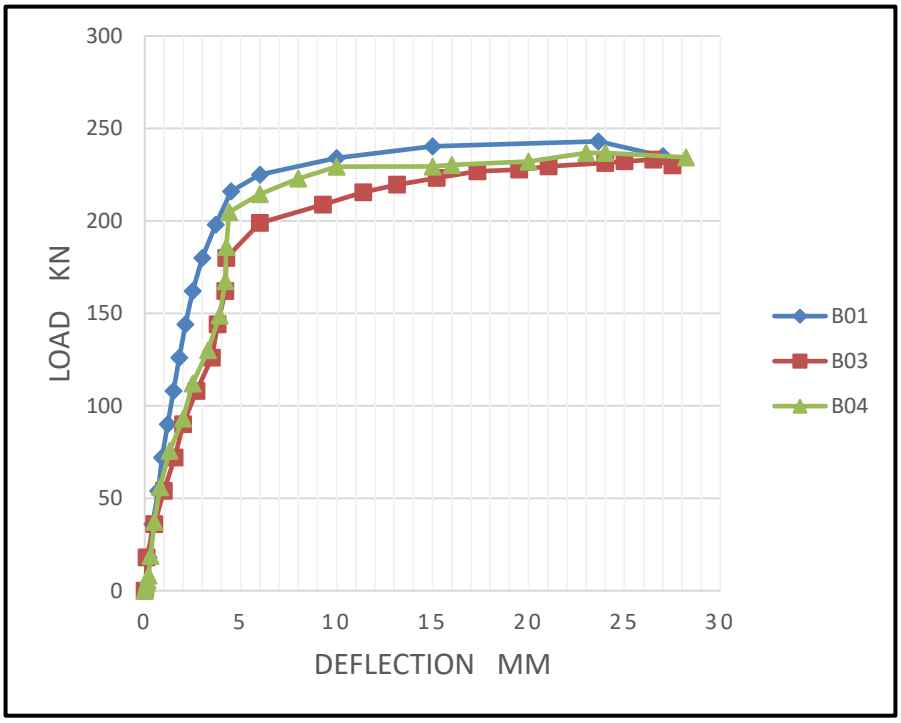

(a)

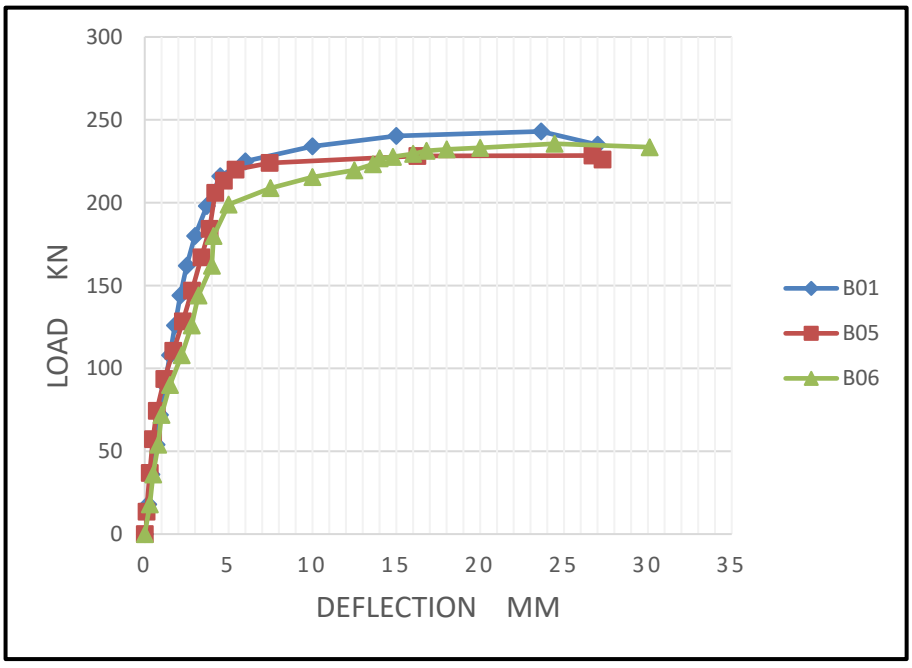

(b)

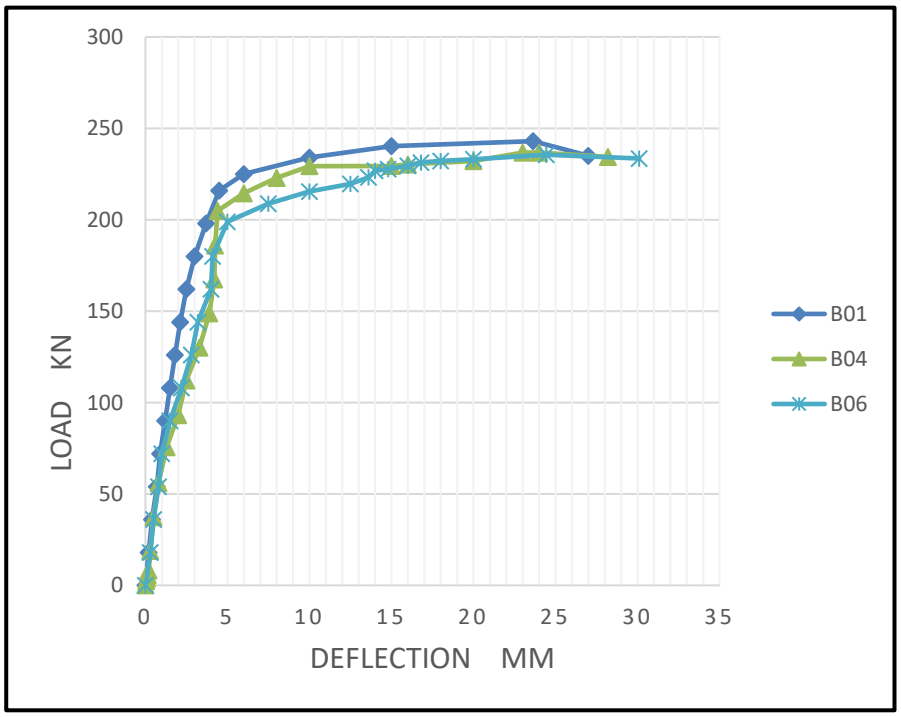
300
250
200
150
100
50
0
LOAD KN
0
5
10
15
20
25
30
35
DEFLECTION MM
B01
B04
B06

(c)

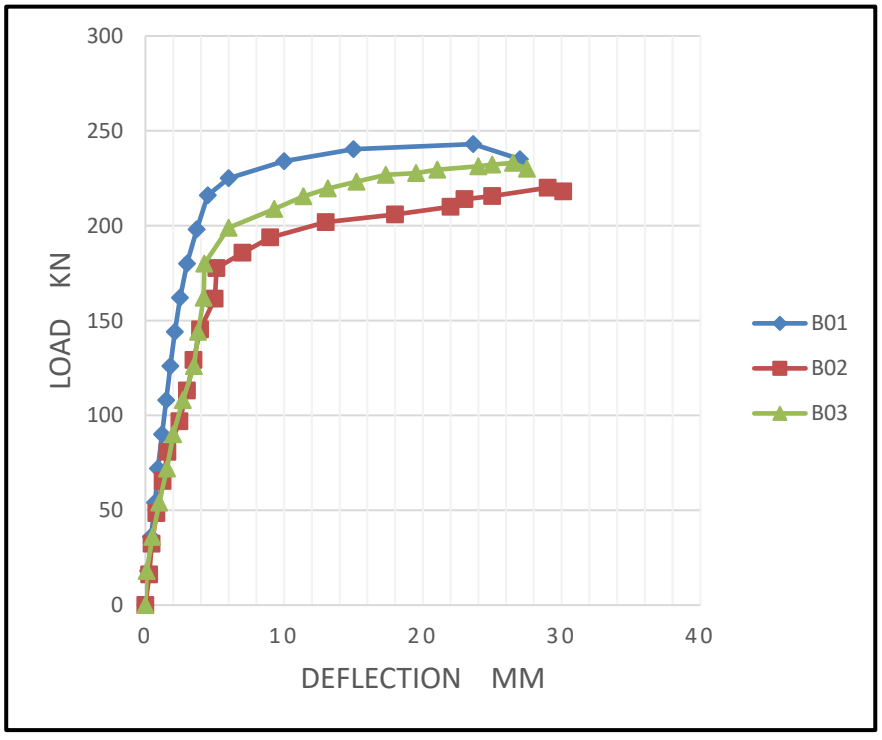
300
250
200
150
100
50
0
LOAD KN
0
10
20
30
40
DEFLECTION MM
B01
B02
B03

(d)

Fig. 7. Load–Mid-span deflection measured for tested beams with different parameters: (a) Equally distributed connectors along span; (b) Connectors concentrated at ends and uniform at mid-span; (c) Uniform, concentrated, and varied-diameter connectors; (d) Beam with vs. without shear connectors.

3.2.2 Horizontal deflection Characteristics

Figures **8a, 8b, 8c, and 8d** illustrate the horizontal deformation between the two layers of the tested beams, revealing several important observations. A comparison between beams with equally distributed and concentrated shear connectors shows that those using Ø8 mm connectors at closer spacing exhibited significantly less horizontal shear deformation than those with Ø10 mm connectors spaced farther apart. This occurred despite both configurations having the same total shear connector area. The reduced deformation in the Ø8 mm connector beams can be attributed to their denser and more concentrated arrangement, which enabled more effective load transfer and minimized slip between the layers. As a result, these beams displayed increased stiffness and improved overall structural behavior. Further comparison between beams B02 and B03 up to failure highlights the critical role of shear connectors. Beam B03, which incorporated shear connectors, demonstrated a more efficient load-bearing response. The connectors helped evenly distribute the load between the two layers, reducing stress concentrations, limiting deflections, and ensuring effective composite action—allowing both layers to deform in unison. In contrast, beam B02 relied solely on friction between the layers, with no connectors. While friction did provide some load transfer capability, it was relatively ineffective under higher loads, leading to uneven stress distribution and localized concentrations. This friction-based connection allowed greater relative movement between the layers, resulting in larger deflections over time and reduced structural stiffness. Moreover, B02 exhibited lower ductility compared to B03. The absence of shear connectors made the layers more susceptible to sliding and independent deformation, thereby decreasing the beam's capacity to absorb and sustain loads without premature failure.

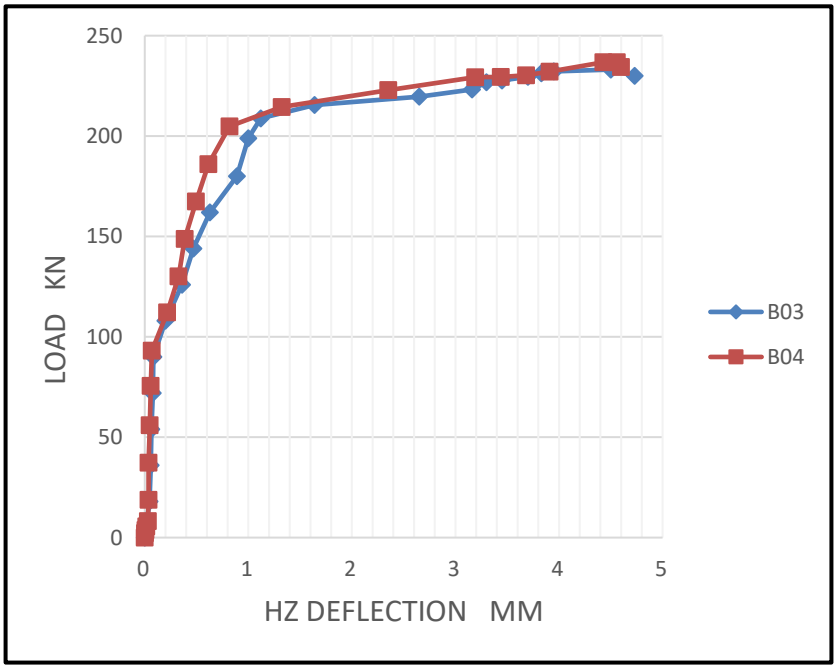

(a)

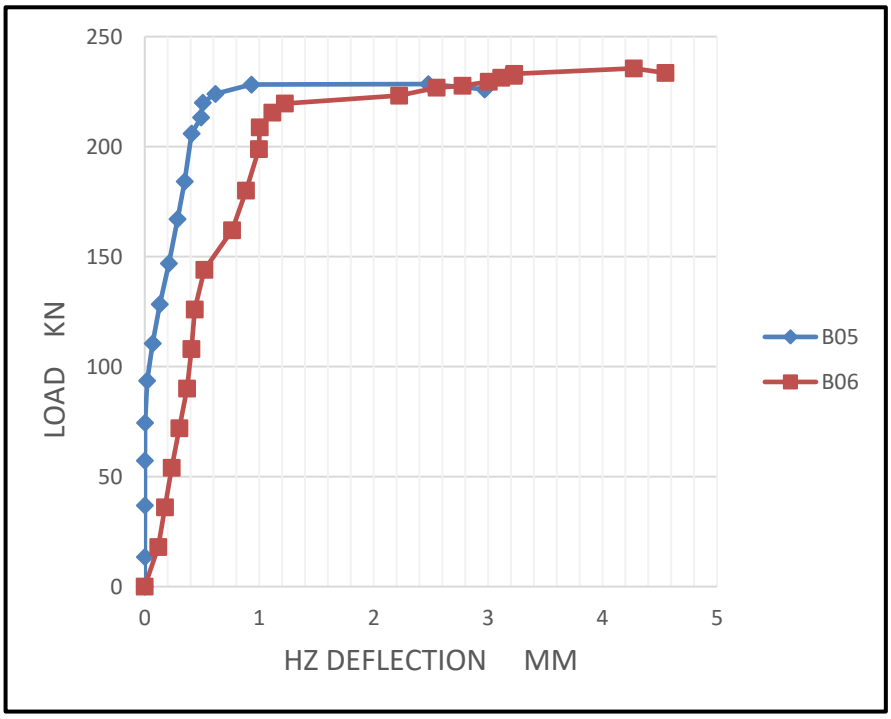
250
200
150
100
50
0
LOAD KN
0
1
2
3
4
5
HZ DEFLECTION MM
B05
B06

(b)

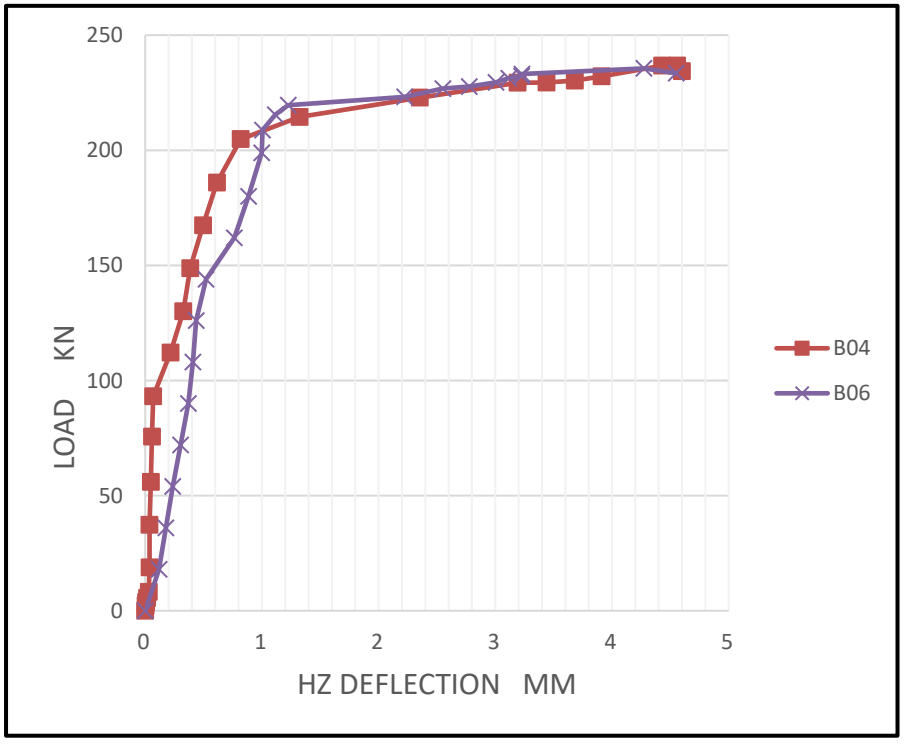
250
200
150
100
50
0
LOAD KN
0
1
2
3
4
5
HZ DEFLECTION MM
B04
B06

(c)

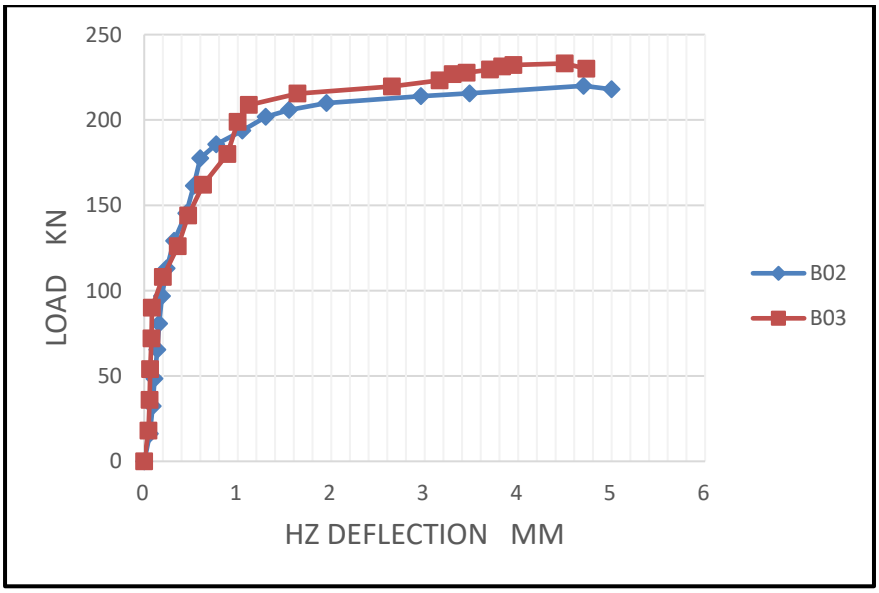

(d)

Fig. 8. Horizontal shear deformation for tested beams with different parameters: (a) Equally distributed connectors along span; (b) Connectors concentrated at ends and uniform at mid-span; (c) Uniform, concentrated, and varied-diameter connectors; (d) Beam with vs. without shear connectors.

3.2.3 Stiffness of specimen

Figure 9 presents the stiffness results for all tested beams. The deflection measured at 70% of the ultimate load showed improvement in beams reinforced with Ø8 mm connectors compared to those with Ø10 mm connectors. Specifically, the stiffness of beams B04 and B06 increased by 3.5% and 4.2%, respectively, when compared to beams B03 and B05. These findings highlight the importance of the number of shear connectors at the interface between the overlay and the substrate, as a higher quantity enhances the transfer of shear stresses and contributes to improved structural stiffness.

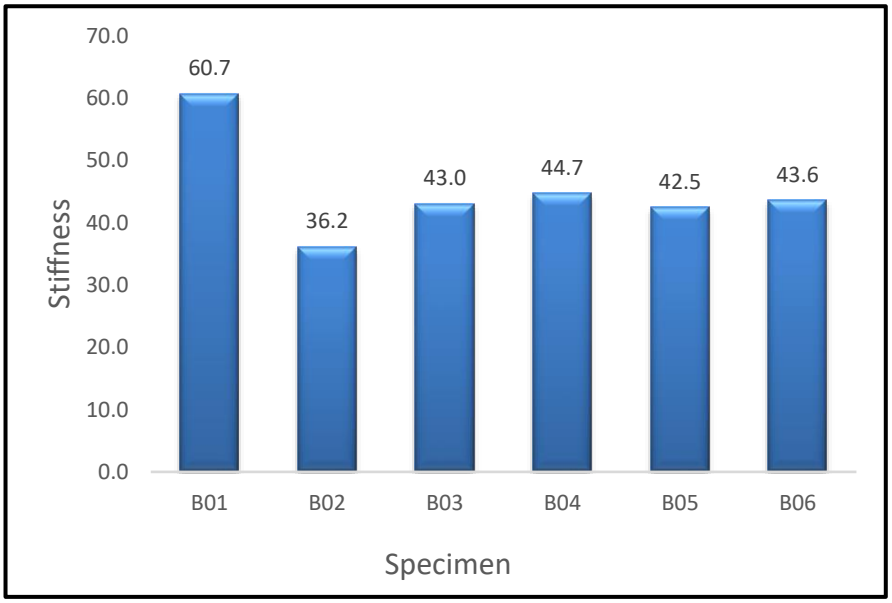

Fig. 9. Stiffness of tested beams.

4 Theoretical Study and Comparison to Design Codes

This section summarizes a thorough investigation of the interface behavior of composite beams to assess the common equations in Proposed Model, ACI and AASHTO LRFD (AASHTO 2018) for calculating the interface shear stress, including the following:

(1) Mast's Shear-Friction Equation (1958):

Mast [18] introduced a linear shear-friction equation, later refined by Anderson in 1960 [19]. The equation is given as:

$$V_n = \rho_v . f_y . \mu \quad \text{eq. (2)}$$

In this context, μ represents the coefficient of friction at the interface, $\rho_v \cdot f_\gamma$ indicates the clamping stress provided by the vertical reinforcement, and v_n denotes the horizontal shear strength.

(2) Shaikh's Equation for Shear Capacity (1978):

Shaikh [20] developed an equation for interfacial shear capacity, which was later adopted by PCI [24] as the basis for design calculations:

$$v_u = \phi . \rho . f_y . \mu \quad \text{eq. (3)}$$

$$\mu_e = (6.90\ \lambda\ \mu)/vu \quad \text{eq. (4)}$$

where $\phi = 0.85$ for shear, $\lambda = 1.0$ for normal weight concrete, 0.85 for sand lightweight concrete, and 0.75 for all lightweight concrete

(3) Loov's Equation for Clamping Stresses (1994):

Loov et al. [21] formulated an equation applicable to both high and low clamping stresses:

$$vu = k.\lambda\ ((0.1+\rho\ f_y)\ fc\ )0.5 \quad \text{eq. (5)}$$

where k = 0.6 for monolithically placed concrete and 0.5 for concrete cast against hardened concrete with a rough surface.

(4) Patnaik's Variation on Horizontal Shear Equations (2001):

Patnaik [22] introduced a linear variation of his earlier horizontal shear equations, noting that a smooth interface without reinforcement may still offer nominal shear strength, though this is not recommended for design purposes:

$$vu = 0.6 + \rho.f_y\ (MPa). \quad \text{eq. (6)}$$

$$vu = 0,\ \rho.f_y < 0.35\ MPa \quad \text{eq. (7)}$$

(5) AASHTO LFRD —The design code states that the horizontal shear Equations (2018) [15]:

The nominal shear resistance of the interface plane shall be taken as:

$$vu = cA_{cv} + \mu\ (\rho_v\ f_v + Pc) \leq v_{umax} \quad \text{eq. (8)}$$

Here, c refers to the cohesion coefficient, with a value of 1.9 MPa for rough interfaces and 0.52 MPa for smooth ones. μ denotes the friction factor, set at 1.0 for rough surfaces and 0.6 for smooth surfaces. P_c represents the permanent net compressive force, while Acvis the area of the concrete shear interface. For design purposes, an upper limit of 0.3f′cand 9.0 MPa is recommended for rough interfaces, and 0.2f′cand 5.5 MPa for smooth interfaces.

(6) American Concrete Institute (ACI) (2019) [16]:

$$V_{nh} = 80 b_v d \qquad \text{eq. (9)}$$

In this context, V_{nh} represents the nominal horizontal shear strength in pounds (lb), bv is the width of the cross-section at the interface being evaluated for horizontal shear (in inches), and d denotes the distance from the extreme compression fiber of the entire composite section to the centroid of the longitudinal tension reinforcement (including both prestressed and non-prestressed steel, if present). For prestressed concrete members, d should not be taken as less than 0.80 times the total section height (h), where h is the overall depth of the composite section, measured in inches.

The horizontal shear stress is found by dividing the shear force by b_{vd} thus resulting in:

$$v_{nh} = 80 \text{ psi} \qquad \text{eq. (10)}$$

The value of the horizontal shear stress is constant for any contact surface width or depth from the extreme compression fiber to the centroid of the tension reinforcement.

(7) Canadian Highway Bridge Design Code (CSA S6-19) [17]:

It is stated that when a crack is assumed to form along the shear plane, the resulting relative displacement is resisted by both cohesion and friction, which are maintained by the shear-friction reinforcement intersecting the crack. In the absence of a more detailed analysis, the shear resistance along the plane, denoted as vr, can be estimated using Equation (11).

$$v_r = \phi c\,(c + \mu\sigma) \qquad \text{eq. (11)}$$

However, the value of vr must not exceed the lesser of 0.25ϕcf′c or 6.5 MPa. Additionally, the values of c (cohesion) and μ (friction factor) are defined as follows:

1. For concrete cast against hardened concrete where the surface is clean and free of laitance but not intentionally roughened, c is taken as 0.25 MPa (0.036 ksi) and μ is $0.60\lambda_1$.
2. For concrete cast against hardened concrete with a clean, laitance-free surface that is *intentionally roughened* to a depth of about 5 mm and spacing of approximately 15 mm, c is 0.50 MPa and μ is $1.0\lambda_1$.
3. For *monolithically placed* concrete, c is 1.00 MPa, and μ is $1.4\lambda_1$.

The factor λ_1, which accounts for concrete density, is defined as:

- 1.0 for normal-density concrete,
- 0.85 for semi-low-density concrete, and
- 0.75 for low-density concrete.

The value of σ shall be calculated as expressed in Eq. (12)

$$\sigma = \rho_v \varepsilon_f E_f + N/A_{cv}$$

where $\varepsilon_f = 0.004$; and $\rho_v = A_{vf}/A_{cv} \geq 0.44\%$. eq. (12)

Table 5: Maximum Interfacial Shear Failure Load from Existing Models and Codes Compared to Experimental Values

	B03 Ø10@400 mm Equal distribution along the beam (kN)		B04 Ø8@150 mm Equal distribution along the beam (kN)		B05 Ø10@300/500 mm Concentration at supports (kN)		B06 Ø8@100/200 mm Concentration at supports (kN)	
Experimental results	233.1		236.8		228.4		235.6	
National building codes	212	9.1%	226	4.56%	212	7.18%	226	4.07%
Mast equation	90	61%	102	57%	90	60.6%	102	56.7%
Birkeland equation [25]	228	2.2%	244	-3.04%	228	0.175%	244	-3.56%
Walraven equation [26]	253	-8.54%	268	-13.2%	253	-10.77%	268	-13.75%
Loov equation [27]	201	13.77%	214.4	9.5%	201	12%	214.4	9%
Shaikh equation	200	14.20%	212	10.5%	200	12.43%	212	10%
Loov and Patnaik equation	206	11.62%	220	7.1%	206	9.8%	220	6.62%

Errors= (Experimental Result-Analysis result) x100 / Experimental result

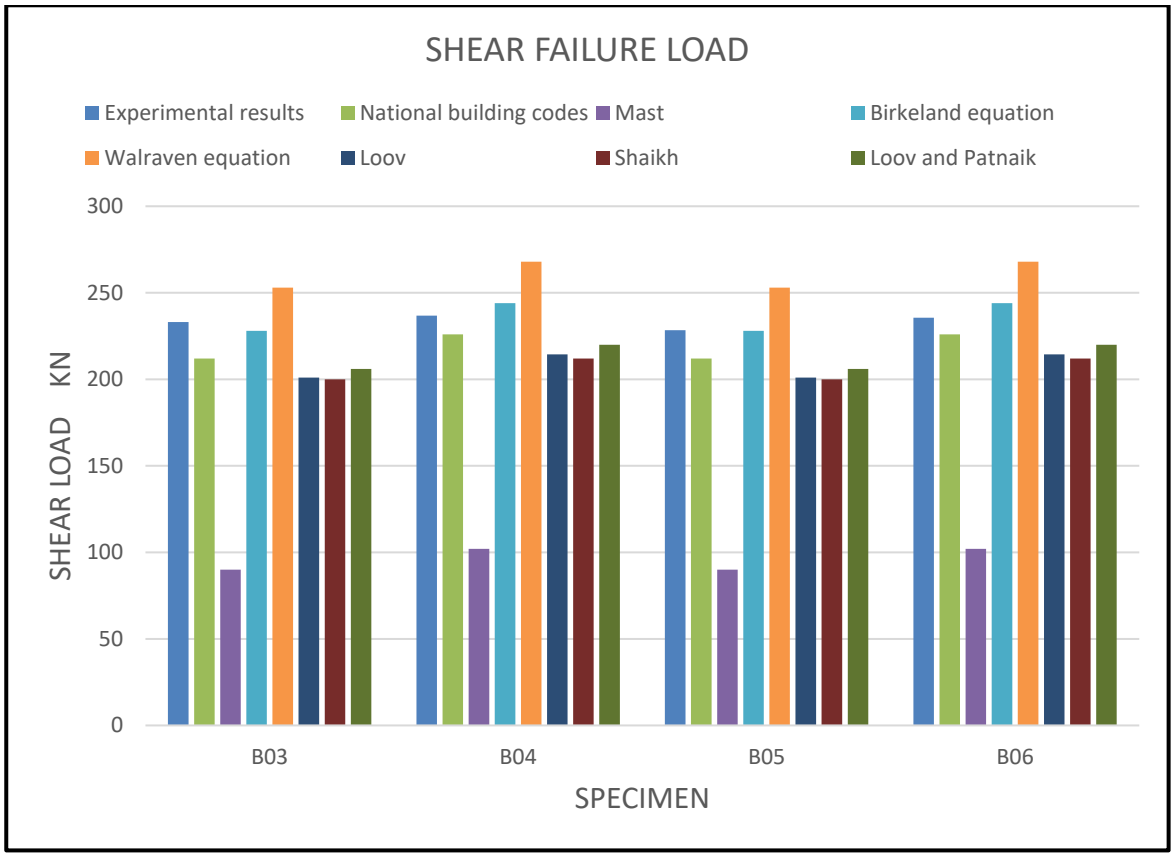

Fig. 10 Results calculated from previous research and codes compared to experimental results.

Shear transfer failure loads were estimated using a range of established analytical models and design codes, and these predictions were compared to the experimental results. A summary of the calculated interfacial shear failure loads and their corresponding experimental values is presented in Table 5. The comparison indicates a strong agreement between the experimental data and the predictions made by the selected design codes and the proposed model. However, deviations ranging from 2% to 60% were noted when comparing experimental results with predictions from other existing models. Figure 10 illustrates a graphical comparison of the interfacial shear failure loads from various models and codes against the experimental results, emphasizing the proposed method's accuracy and effectiveness in capturing actual shear transfer behavior.

Conclusions

This study investigates the interfacial shear behavior of composite concrete beams, focusing on the influence of shear connector distribution along the beam span.

(1) The analysis confirmed that beams strengthened with bonded concrete overlays demonstrated significantly improved behavior, with ultimate load capacities and stiffness values approaching those of monolithic beams. This indicates effective composite action between the original and overlay layers.

(2) The experimental findings emphasized the critical role of shear connectors in enhancing the structural response of strengthened beams and in mitigating the risk of interfacial debonding.

(3) Incorporating steel dowels across the interface notably improved the shear transfer capacity, minimized crack widths, and led to a more favorable failure mode when compared to beams strengthened through friction only.

The main findings are as follows:

- **Effect of Shear Connector Diameter:**

When maintaining the same total steel area for shear connectors, beams using smaller-diameter connectors demonstrate superior bonding and stiffness compared to those with larger-diameter connectors. This advantage is evident whether the connectors are evenly spaced along the beam span or concentrated at the ends. The improvement results from the closer spacing between the smaller connectors, which enhances the interface contact. The most notable gains include a 3.3% increase in yield load and a 3.1% rise in ductility factor, along with a 2.4% boost in ultimate load capacity, although these improvements are relatively modest.

- **Influence of Shear Connector Distribution:**

Focusing shear connectors near the supports improves ductility more effectively than distributing them evenly along the beam span. This is because slip between the layers is minimal at mid-span but peaks near the beam ends. By placing connectors at the ends, interfacial clamping is enhanced, resulting in better ductility. Concentrating connectors causes only a negligible decrease in ultimate load capacity (–0.4% for Pult and –0.5% for Pmax), showing that strategic reinforcement placement can maintain similar load capacity while potentially optimizing material use. Both distribution methods display nearly identical deflection behavior, with concentrated connectors allowing slightly higher ultimate deflection (+1.7%) while yield deflection remains the same, indicating similar stiffness despite different layouts. However, a 3.2% reduction in yield load was noted for the concentrated arrangement, suggesting that uniform distribution offers slightly better initial resistance to failure. The concentrated connectors also achieved a modest 1.5% increase in ductility factor, reflecting comparable post-yield deformation and energy dissipation capabilities.

- **Comparison Between beam with vs. without shear connectors**

Beams equipped with shear connectors exhibit greater ductility, improved load distribution, and increased stiffness compared to those that depend only on friction. The ductility factor shows a notable improvement of 16.4%, which significantly boosts structural safety and reliability. Additionally, there is a 7.3% rise in ultimate load capacity and a 12.0% decrease in yield deflection. The uniform failure mode observed across the specimens suggests that shear connectors not only enhance performance but also ensure consistent and predictable structural behavior.

References

[1] Zaky,W. and M.Rabie., “Effect of cases of loading and distribution of shear connectors on the behavior of One -Way composite pre-slabs”, Life Science Journal, Vol. 9, No. 2, 2012. pp. 435-443.

[2] Abd El-Hay A.S. (2006) Shear transfer in composite continuous one-way pre-slabs. PH. D Thesis. Faculty of Engineering, Cairo University.

[3] Waleed A. Thanoon, Yavuz. Yardim, M.S. Jaafar, J, Noorzaei., “Development of interlocking mechanism for shear transfer in composite floor”, Construction and Building Materials Journal, Vol.24,2010, pp.2604-2611

[4] Abdel-Wahab, H. M., and Khalil, M. H., “Rigidity and strength of orthotropic reinforced concrete waffle slabs”, ASCE, Vol. 126, No. 2, February, 2000. pp. 219-227.

[5] Abou El-Maaty, M. A., “Composite corrugated Precast reinforced concrete deck slabs”, PH. D thesis. Faculty of Engineering. Cairo Univ. 1997.

[6] Dong-Uk choi, David, W.F., and jomaso, J., "Interface shear strength of concrete at early ages", ACI structural journal, Vol. 96, No. 3, May-June 1999, pp. 343-347.
[7] Easterling, W. S., and Young, C. S., "Strength of composite slabs", Journal of structural Engineering ASCE, Vol. 118, No. 9, September, 1992. pp. 2370-2389.
[8] El-Behairy, Sh., and Abu El-Enin, A. W., "Behavior of simply supported pre-slab system", Bulletin No. 15-C20, 1984, Faculty of Engineering, Ain Shams Univ.
[9] El-Zanaty, A. (1995), "Shear transfer behavior of initially cracked concrete with compressive stresses normal to the shear plane", Egyptian society of Engineers, Vol. 34, No. 1.
[10] IHAB Abdallah Hussien, "Effect of shear connectors on composite concrete beams", M.sc. Thesis. Faculty of Eng. Cairo Univ. 1991.
[11] Elsayed., "Behavior of simply supported high strength concrete composite T-beams", M.sc. Thesis. Faculty of Engineering Cairo Univ., 2002
[12] Nawy, E. G., Ukadile, M. M., and Balaguru, P. N., "Investigation of concrete: PMC composite", Journal of the structural division, ASCE, Vol. 108, No. ST-5, May 1982. pp. 1049-1063.
[13] Saemann, J. C., and Washa, G., "Horizontal shear connections between precast beams and cast-in place slabs", ACI, Nov. 1964. pp. 1383-1404.
[14] M.Rabie., "Shear transfer in composite reinforced concrete sections", PH. D Thesis. Faculty of Engineering. Cairo Univ. 1994.
[15] AASHTO, 2018, "AASHTO LRFD Bridge Design Specifications for GFRP-Reinforced Concrete," second edition, American Association of State Highway Transportation Officials, Washington, DC, 14 pp.
[16] ACI Committee 318, 2019, "Building Code Requirements for Structural Concrete (ACI 318-19) and Commentary (ACI 318R-19) (Reapproved 2022)," American Concrete Institute, Farmington Hills, MI, 624 pp.
[17] CAN/CSA S6-19, 2019, "Canadian Highway Bridge Design Code," CSA Group, Toronto, ON, Canada.
[18] R.F. Mast, Auxiliary reinforcement in concrete connections, Proceedings of ASCE Journal 94 (ST6) (1968) 1485–1504.
[19] R.A. Anderson, Composite designs in precast and cast-in-place concrete, Progressive Architecture 41–49 (1960) 172–179.
[20] A.F. Shaikh, Proposed revisions to shear-friction provisions, PCI Journal 23 (2) (1978) 12–21.
[21] R.E. Loov, A.K. Patnaik, Horizontal shear strength of composite concrete beams with a rough interface, PCI Journal 39 (1) (1994) 48–69.
[22] A.K. Patnaik, Behavior of composite concrete beams with smooth interface, Journal of Structural Engineering 127 (4) (2001) 359–366.
[23] M. Awry, T. El-Afandy, H. Okail, A. Abdelrahman, Rehabilitation of composite concrete RC beams deficient in interfacial shear transfer, Azhar Journal (2013).
[24] PCI Design Handbook – Precast and Prestressed Concrete, 4th ed., Precast/Prestressed Concrete Institute, Chicago, IL, 1992.
[25] P.W. Birkeland, H.W. Birkeland, Connections in pre-cast concrete construction, ACI Journal 63 (3) (1966) 345–367.
[26] J. Walraven, J. Frenay, A. Pruijssers, Influence of concrete strength and load history on the shear friction capacity of concrete members, PCI Journal 32 (1) (1987) 66–84.
[27] R.E. Loov, ''Design of Precast Connections'', Paper Presented at a Seminar Organized by Compa International Pte Ltd, September 25–27, Singapore, p. 8.
[28] Yang Song, Shuwen Yao and Long Liu 2, Flexural Reinforcement of Over-Reinforced Beam by Ultrahigh Performance Concrete Layer, Hindawi Mathematical Problems in Engineering Volume 2022, Article ID 9171300, 15 pages.
[29] Liu, T.; Charron, J.-P. Characterization of interface properties for modeling the shear behavior of T-beams strengthened with ultra-high-performance concrete. In Structure and Infrastructure Engineering; [30] Taylor & Francis: Abingdon, UK, 2023; pp. 1–16.
[30] Liu, T.; Charron, J.-P. Experimental study on the shear behavior of UHPC-strengthened concrete T-beams. J. Bridge Eng. 2023, 28, 04023064.